Novel Energy Harvesting AF Relaying Schemes With Channel Estimation Errors

Yulin Zhou, Yunfei Chen, *Senior Member,IEEE*

***Abstract*—Three novel structures using simultaneous wireless information and power transfer in energy harvesting amplify-and-forward(AF) relaying are investigated in this paper. Different combinations of time-switching (TS) and power-splitting (PS) energy harvesting protocols are studied. Three dynamic schemes are proposed as channel estimation power splitting (CEPS), data transmission power splitting (DTPS) and combination power splitting (CPS). From source to relay (SR) in these schemes, the data packet includes three parts: channel estimation, data transmission and energy harvesting. From relay to destination (RD) in these schemes, the data packet includes two parts: data transmission and channel estimation. Closed-form expressions for the cumulative distribution function (CDF) of the end-to-end signal-to-noise ratio (SNR) for the three structures are derived. Using these expressions, achievable rate (AR) and bit-error-rate (BER) are derived. Different parameters are examined. Numerical results show the optimal splitting ratio for channel estimation, energy harvesting and data transmission, when the packet size is fixed.**

***Index Terms*—Amplify-and-forward, channel estimation, energy-harvesting, power-splitting (PS) protocol, relaying-systems, time-switching (TS) protocol.**

I. INTRODUCTION

Relays have been considered in many communication systems due to their ability to improve reliability. Relaying mainly contains decode-and-forward (DF) and amplify-and-forward (AF). AF relaying is commonly used to increase the system reliability [1]–[4]. At the AF relay, the amplification and forwarding operations consume extra energy, which limits lifetime of devices relying on batteries, such as sensors used in buildings or human bodies [5]. Therefore, radio frequency (RF) energy harvesting (EH) has been studied as an appropriate solution [1]. The information signal received by the relay is sent to the destination using the energy harvested from the source [6]. For example, the artificial-noise-aided secure beamforming design with energy harvested from the source have been discussed in [7], [8], and the nonlinear conversion efficiency for energy harvester in EH wireless systems has been studied in [9], [10]. Since RF signals can be used for both information decoding (ID) and EH at the same time, EH can provide extra energy in signal processing [11]. In [2], two different energy harvesting protocols have been proposed: power-splitting (PS) and time-switching (TS). The harvest-use structures were used for either TS or PS in [12]. In [13], more advanced energy harvesting structures have been discussed, where the authors analyzed the rate-energy tradeoff for wireless information and power transfer. Non-linear energy harvesting using four practical simultaneous wireless information and power transmission structures was first developed in [14]. In these schemes, EH is an important part of relaying to prolong the lifetime of the relay node for sustainable operations. PS reduces the information decoding power at the relay, while TS reduces the throughput. The efficiency of energy harvesting relaying can be further improved by considering them jointly, which has inspired us to develop combination structures using both TS and PS.

Another important part of wireless relaying is channel estimation, which is necessary for demodulation at the destination. For variable-gain AF relaying, both relay and destination require channel estimation. Channel estimation has been studied in several previous works. For instance, in [15], linear minimum mean squared error (LMMSE) estimator was proposed. In [16], minimum mean squared error (MMSE) estimators were studied. In [17], estimators for individual channel coefficients were studied, and moment-based (MB) estimators were developed in [18] for individual channel power. In [19], the performances of different channel estimators in AF relaying with energy harvesting were compared. These estimators were developed for AF relaying without RF EH, where the pilots for channel estimation are sent from relay to destination using the relay's own power, in addition to the data transmission power.

In this paper, three novel structures of EH AF relaying are proposed. The relay network model is shown in Fig. 1 and the data packets for different structures are shown in Fig. 2. In these structures, the pilots are sent from relay to destination by using the energy harvested from the source without using the relay's own power. To improve the efficiency of energy harvesting, different combinations of time-switching (TS) and power-splitting (PS) in the first hop have been considered. The optimal power allocation among different parts of the data packet, that is, channel estimation, energy harvesting and information decoding, is explored. The data packet in the second hop contains channel estimation and information decoding. Compared with the previous works, the main difference between this work and [12] is that [12] considered TS and PS separately, while this work considers different combinations of TS and PS simultaneously. Compared with [13], this work includes channel estimation and information decoding and the harvested energy is used for both information decoding and channel estimation, while [13] only considered channel estimation. Our structures consider all factors mentioned in previous works at the same time, which makes our design more comprehensive.

Two contributions of this work are summarized as follows. Firstly, this is the first work on AF relaying that considers

Yulin Zhou is with School of Engineering, University of Warwick, Coventry, U.K. CV4 7AL, e-mail: Yulin.Zhou@warwick.ac.uk.

Yunfei Chen is with School of Engineering, University of Warwick, Coventry, U.K. CV4 7AL, e-mail: yunfei.chen@warwick.ac.uk.

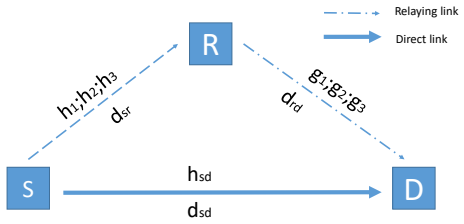

Fig. 1. AF relaying network.

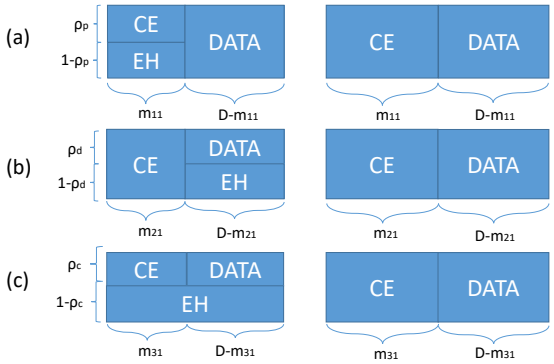

Fig. 2. (a) Channel estimation power splitting (CEPS) structure; (b) Data transmission power splitting (DTPS) structure; (c) Combination power splitting (CPS) structure.

data packets with channel estimation, EH and information decoding. In the previous works, either the use of EH in information decoding or the use of EH in channel estimation were considered but not both. Secondly, the cumulative distribution function (CDF) of the end-to-end signal-to-noise ratio (SNR) for the three novel energy harvesting structures are derived in this paper. These functions allow the derivation of the achievable rate and bit error rate as well as the optimal power allocation. The structures presented in this work can be further used as the basic EH AF relaying protocols.

II. SYSTEM MODEL

Fig. 1 shows the AF relaying network including a source S, a relay R and a destination D. Let d_{sr}, d_{rd}, d_{sd} denote the distances between S and R, R and D and S and D, respectively. Denote h_1, h_2 and h_3 as the fading gains for different structures in the channel between the source and the relay and are complex Gaussian with mean zero and variance $2\theta^2$. Denote g_1, g_2 and g_3 as the fading channel coefficients of the relay-to-destination links and are complex Gaussian random variables with mean zero and variance $2\theta^2$. Fig. 2(a) shows the channel estimation power splitting (CEPS) structure. Using PS, the source sends m_{11} pilots using its own power, each of which is split in power with power ratio ρ_p for EH and $(1-\rho_p)$ for channel estimation, while the data is added using TS. Note that these pilots are not sent by using the harvested power in this case. Fig. 2(b) shows the data transmission power splitting (DTPS) structure. In this structure, the source sends m_{21} pilots for channel estimation, and the data symbols are split in power with power ratio ρ_d for EH and $(1-\rho_d)$ for data transmission. Fig. 2(c) shows the combined power splitting (CPS) structure. In this structure the source sends m_{31} pilots for channel estimation and $(D-m_{31})$ data symbols for information delivery. The energy is harvested by splitting all symbols for both channel estimation and data transmission with power splitting ratio ρ_c.

Each node is equipped with a single antenna and works in half-duplex. There are two hops: source-to-relay (SR) link and relay-to-destination (RD) link. The following assumptions are used in this paper.

A. Assumptions

1) Time division is used in all the structures to achieve orthogonal channels. Therefore, the source first sends the data packet to the relay, and then the relay sends the data packet to the destination.
2) A total of D symbols are used in each structure for channel estimation, data transmission and energy harvesting. Each symbol occupies a time duration of T seconds.
3) All fading channel coefficients are complex Gaussian random variables with mean zero, which are fixed for each data packet but vary from packet to packet.
4) Variable-gain relaying is assumed so that the amplification factor changes with the estimated channel gain in the SR link [20], [21].
5) All the values of m_{11}, m_{21} and m_{31} in Fig. 2 are integers and smaller than D. Also, $0 \leqslant \rho_p, \rho_d, \rho_c \leqslant 1$.
6) The conversion efficiency from AC to DC is assumed constant.

B. Signal Models

Next, we give the signal models for different structures.

1) CEPS: In the CEPS structure, there are three parts in the first hop: pilots for channel estimation and energy harvesting, and data symbols for data transmission. At the relay, the received signals of the m_{11} pilots are split into two parts with a power splitting factor $0 < \rho_p < 1$. First, the received pilot at relay for channel estimation is given by

$$y_r[i_{11}] = \sqrt{\frac{\rho_p P_{s1}}{d_{sr}^{\ e}}} h_1 x[i_{11}] + n_{11}[i_{11}] \tag{1}$$

where $i_{11} = 1, 2, \ldots, m_{11}$ is the total number of pilots in the data packet, $0 < m_{11} < D$ is an integer, P_{s1} is the transmitted power of the source, d_{sr} is the distance between source and relay, e is the path loss exponent, $x[i_{11}]$ is the transmitted pilot with unit power $E\{|\, x[i_{11}]\,|^2\} = 1$, $E\{.\}$ represents the expectation operator, and $n_{11}[i_{11}]$ is the complex AWGN with mean zero and noise power N_{11}.

The received signal of the data symbols can be expressed as

$$y_r[j_{11}] = \sqrt{\frac{P_{s1}}{d_{sr}^{\ e}}} h_1 x[j_{11}] + n_{11}[j_{11}] \tag{2}$$

where $j_{11} = m_{11}+1, \ldots, D$, $x[j_{11}]$ is the transmitted data symbol with unit power $E\{|\, x[j_{11}]\,|^2\} = 1$, $n_{11}[j_{11}]$ is the

complex AWGN with mean zero and noise power N_{11}. This power is supplied by source, not the harvester.

Hence, the harvested energy at the relay is

$$E_{r1} = \frac{\eta P_{s1} |h_1|^2 (1-\rho_p) m_{11}}{{d_{sr}}^e} \tag{3}$$

where η stands for the conversion efficiency of the energy harvester and we have assumed $T = 1$ for simplicity. The harvested energy will be used to transmit m_{11} pilots to the destination for the channel estimation and $D - m_{11}$ data symbols from the source in the second hop to keep the same data rate. Thus the transmission power of the relay is

$$P_{r1} = \frac{\eta P_{s1} |h_1|^2 (1-\rho_p) m_{11}}{D {d_{sr}}^e}. \tag{4}$$

Using (1), we can get an estimate of h_1 as

$$\hat{h_1} = \frac{\Sigma_{i_{11}=1}^{m_{11}} [\sqrt{\rho_p P_{s1}} h_1 + n_{11}[i_{11}]]}{m_{11} \sqrt{\frac{\rho_p P_{s1}}{{d_{sr}}^e}}} = h_1 + \varepsilon_{11} \tag{5}$$

where $\varepsilon_{11} = \frac{\Sigma_{i_{11}=1}^{m_{11}} n_{11}[i_{11}]}{m_{11} \sqrt{\frac{\rho_p P_{s1}}{{d_{sr}}^e}}}$ is the estimation error. Thus, one has $h_1 = \hat{h_1} - \varepsilon_{11}$.

The received signal in (2) is amplified-and-forwarded to the destination by using the harvested energy in (3) and the channel estimate in (5). Thus, the amplification factor can be written as

$$\hat{a}_{1var}^2 = \frac{1}{\frac{P_{s1} |\hat{h_1}|^2}{{d_{sr}}^e} + N_{11}} \tag{6}$$

where $\hat{h_1}$ is the estimated channel gain for the first hop between source node and relay node in (5).

During the second hop, the received pilots for channel estimation at the destination node can be written as

$$y_d[i_{12}] = \sqrt{\frac{P_{r1}}{{d_{rd}}^e}} g_1 \hat{a}_{1var} x[i_{12}] + n_{12}[i_{12}] \tag{7}$$

where $i_{12} = 1, 2, \ldots, m_{11}$, $x[i_{12}]$ is the pilot value, $n_{12}[i_{12}]$ is the AWGN with zero-mean and noise power N_{12}, $\hat{a}_{1var}$ is the amplification factor given in (6), P_{r1} is the relay transmission power given in (4), d_{rd} is the distance between relay and destination.

Also, the received data symbols at the destination can be expressed as

$$y_d[j_{12}] = \sqrt{\frac{P_{r1}}{{d_{rd}}^e}} g_1 \hat{a}_{1var} \left(y_r[j_{11}]\right) + n_{12}[j_{12}] \tag{8}$$

where $n_{12}[j_{12}]$ is additive white Gaussian noise (AWGN) at the destination node with zero mean and noise power N_{12}, and all the other symbols are defined as before.

The received data symbols at the destination in the direct link can be expressed as

$$y_d[j_{11}] = \sqrt{\frac{P_{s1}}{{d_{sd}}^e}} h_{sd} x[j_{11}] + n_{sd}[j_{11}] \tag{9}$$

where d_{sd} is the distance between source and destination, and $n_{sd}[j_{11}]$ is the complex AWGN with mean zero and noise power N_{sd}.

2) DTPS: The DTPS structure is similar to CEPS, except that energy is harvested from the data symbols.

First, the pilots received at the relay for channel estimation in the first hop is

$$y_r[i_{21}] = \sqrt{\frac{P_{s2}}{{d_{sr}}^e}} h_2 x[i_{21}] + n_{21}[i_{21}] \tag{10}$$

where $i_{21} = 1, 2, \ldots, m_{21}$, m_{21} is the number of pilots used for channel estimation, P_{s2} is the transmitted power of the source, $x[i_{21}]$ is the transmitted pilot with unit power $E\{|\, x[i_{21}]\,|^2\} = 1$, and $n_{21}[i_{21}]$ is the complex AWGN with mean zero and noise power N_{21}.

Also, the received signals of the data symbols in the second part of the data packet in the first hop can be expressed as

$$y_r[j_{21}] = \sqrt{\frac{\rho_d P_{s2}}{{d_{sr}}^e}} h_2 x[j_{21}] + n_{21}[j_{21}] \tag{11}$$

where $j_{21} = m_{21} + 1, \ldots, D$, $x[j_{21}]$ is the data symbol with $E\{|\, x[j_{21}]\,|^2\} = 1$, $n_{21}[j_{21}]$ is the complex AWGN during data reception at the relay with zero-mean and noise power N_{21}.

The transmission power of the relay is

$$P_{r2} = \frac{\eta P_{s2} |\hat{h_2}|^2 (1-\rho_d)(D - m_{21})}{D {d_{sr}}^e}. \tag{12}$$

Using (10), we estimate h_2 as

$$\hat{h_2} = h_2 + \varepsilon_{21} \tag{13}$$

where $\varepsilon_{21} = \frac{\Sigma_{i_{21}=1}^{m_{21}} n_{21}[i_{21}]}{m_{21} \sqrt{\frac{P_{s2}}{{d_{sr}}^e}}}$ is the estimation error. Thus, one has $h_2 = \hat{h_2} - \varepsilon_{21}$.

The received data in (11) is sent to the destination by using the transmission power of the relay in (12) and the channel estimate in (13). Thus, the amplification factor can be written as

$$\hat{a}_{2var}^2 = \frac{1}{\frac{P_{s2}}{{d_{sr}}^e} |\hat{h_2}|^2 + N_{21}}. \tag{14}$$

During the second hop, the received pilots for channel estimation at the destination can be written as

$$y_d[i_{22}] = \sqrt{\frac{P_{r2}}{{d_{rd}}^e}} g_2 \hat{a}_{2var} x[i_{22}] + n_{22}[i_{22}] \tag{15}$$

where $i_{22} = 1, 2, \ldots, m_{21}$ and $x[i_{22}] = 1$ is the pilot value, $n_{22}[i_{22}]$ is the additive white Gaussian noise (AWGN), $\hat{a}_{2var}$ is the amplification factor given in (14), P_{r2} is the relay transmission power given in (12).

Also, the received data symbols at the destination are

$$y_d[j_{22}] = \sqrt{\frac{P_{r2}}{{d_{rd}}^e}} g_2 \hat{a}_{2var} \left(y_r[j_{21}]\right) + n_{22}[j_{22}]. \tag{16}$$

The direct link is still given by (9).

3) CPS: In the CPS structure, energy is harvested by splitting power from both pilot symbols and data symbols.

The pilot received at the relay for channel estimation is

$$y_r[i_{31}] = \sqrt{\frac{\rho_c P_{s3}}{{d_{sr}}^e}} h_3 x[i_{31}] + n_{31}[i_{31}] \tag{17}$$

where $i_{31} = 1, 2, \ldots, m_{31}$, $0 < m_{13} < D$ is the number of pilots used for channel estimation, P_{s3} is the transmitted

power of the source, $x[i_{31}]$ is the transmitted pilot symbol with $E\{x[i_{31}]^2\} = 1$, and $n_{31}[i_{31}]$ is the complex AWGN with mean zero and noise power N_{31}.

The received data symbols can be expressed as

$$y_r[j_{31}] = \sqrt{\frac{\rho_c P_{s3}}{{d_{sr}}^e}} h_3 x[j_{31}] + n_{31}[j_{31}] \tag{18}$$

where $j_{31} = m_{31}+1, \ldots, D$, $x[j_{31}]$ satisfies $E\{|\ x[j_{31}]\ |^2\} = 1$, $n_{31}[j_{31}]$ is the complex AWGN during data reception at the relay with mean zero and noise power N_{31}.

The transmission power of the relay is

$$P_{r3} = \frac{\eta P_{s3} |h_3|^2 (1-\rho_c)}{{d_{sr}}^e}. \tag{19}$$

Using (17), h_3 can be estimated as

$$\hat{h_3} = h_3 + \varepsilon_{31} \tag{20}$$

with $\varepsilon_{31} = \frac{\Sigma_{i_{31}=1}^{m_{31}} n_{31}[i_{31}]}{m_{31}\sqrt{\rho_c \frac{P_{s3}}{{d_{sr}}^e}}}$ and $h_3 = \hat{h_3} - \varepsilon_{31}$.

In this case, the amplification factor can be written as

$$\hat{a}_{3var}^2 = \frac{1}{\frac{P_{s3}}{{d_{sr}}^e} |\hat{h_3}|^2 + N_{31}}. \tag{21}$$

The received pilots for channel estimation at the destination are

$$y_d[i_{32}] = \sqrt{\frac{P_{r3}}{{d_{rd}}^e}} g_3 \hat{a}_{3var} x[i_{32}] + n_{32}[i_{32}] \tag{22}$$

where $i_{32} = 1, 2, \ldots, m_{31}$ denotes the pilots for channel estimation, and $x[i_{32}] = 1$ is the pilot value, $n_{12}[i_{32}]$ is the additive white Gaussian noise (AWGN).

Also, the received data symbols at the destination can be expressed as

$$y_d[j_{32}] = \sqrt{\frac{P_{r3}}{{d_{rd}}^e}} g_3 \hat{a}_{3var} \left(y_r[j_{31}]\right) + n_{32}[j_{32}], \tag{23}$$

where $n_{32}[j_{32}]$ is additive white Gaussian noise (AWGN) at the destination node. The direct link is also given by (9).

III. End-to-End SNR Analysis

In this section, we will derive the end-to-end SNR expressions for different structures. These expressions can be used to analyze the system performances.

1) The CEPS Structure: By using the received signals in (7), the channel gain of the RD link can be estimated as

$$\hat{g_1} = \frac{\Sigma_{i_1=1}^{m_{11}} \left(\sqrt{\frac{P_{r1}}{{d_{rd}}^e}} g_1 \hat{a}_{1var} + n_{12}[i_1]\right)}{m_{11}\hat{a}_{1var}\sqrt{\frac{\hat{P_{r1}}}{{d_{rd}}^e}}} = \frac{\sqrt{\frac{P_{r1}}{{d_{rd}}^e}}}{\sqrt{\frac{\hat{P_{r1}}}{{d_{rd}}^e}}} g_1 + \varepsilon_{12} \tag{24}$$

where $\varepsilon_{12} = \frac{\Sigma_{i_{12}=1}^{m_{11}} n_{12}[i_{12}]}{m_{11}\hat{a}_{1var}\sqrt{\frac{P_{r1}}{{d_{rd}}^e}}}$ and $\hat{P_{r1}} = \frac{\eta P_{s1} |\hat{h_1}|^2 (1-\rho_p) m_{11}}{D {d_{sr}}^e}$.

By using (24) and (5) in (8), the received signal at the destination can be expanded to give the end-to-end SNR expression as

$$\gamma_{1end} = \frac{E[|\sqrt{\frac{\hat{P_{r1}}}{{d_{rd}}^e}} \hat{g_1} \hat{a}_{1var} \sqrt{\frac{P_{s1}}{{d_{sr}}^e}} \hat{h_1} x[j_{11}]|^2]}{u} \tag{25}$$

where $u = E[|\sqrt{\frac{\hat{P_{r1}}}{{d_{rd}}^e}} \hat{g_1} \hat{a}_{1var} \sqrt{\frac{P_{s1}}{{d_{sr}}^e}} \varepsilon_{11} x[j_{11}]|^2]$
$+ E[|\sqrt{\frac{\hat{P_{r1}}}{{d_{rd}}^e}} \hat{g_1} \hat{a}_{1var} n_{11}[j_{11}]|^2]$
$+ E[|n_{12}[j_{12}]|^2] + E[|\sqrt{\frac{\hat{P_{r1}}}{{d_{rd}}^e}} \sqrt{\frac{P_{s1}}{{d_{sr}}^e}} \hat{h_1} \hat{a}_{1var} \varepsilon_2 x[j_{11}]|^2]$
$+ E[|\sqrt{\frac{\hat{P_{r1}}}{{d_{rd}}^e}} \sqrt{\frac{P_{s1}}{{d_{sr}}^e}} \hat{a}_{1var} \varepsilon_{11} \varepsilon_{12} x[j_{11}]|^2]$
$+ E[|\sqrt{\frac{\hat{P_{r1}}}{{d_{rd}}^e}} \varepsilon_{12} \hat{a}_{1var} n_{11}[i]|^2]$.

One has $E[|x[j_{11}]|^2] = 1$, $E[|n_{11}[j_{11}]|^2] = N_{11}$ and $E[|n_{12}[j_{12}]|^2] = N_{12}$. Also, denote $E[|\varepsilon|_1^2] = \varepsilon_{11var}$,$E[|\varepsilon|_2^2] = \varepsilon_{12var}$. Equation (25) becomes

$$\gamma_{1end} = \frac{\frac{P_{s1}}{{d_{sr}}^e} |\hat{g_1}|^2 |\hat{h_1}|^2}{v_1} \tag{26}$$

where $v_1 = \frac{P_{s1}}{{d_{sr}}^e} |\hat{g_1}|^2 \varepsilon_{11var} + |\hat{g_1}|^2 N_{11} + \frac{P_{s1}}{{d_{sr}}^e} \varepsilon_{12var} |\hat{h_1}|^2 + \frac{P_{s1}}{{d_{sr}}^e} \varepsilon_{11var} \varepsilon_{12var} + N_{11}\varepsilon_{12var} + \frac{N_{12}}{\frac{\hat{P_{r1}}}{{d_{rd}}^e} \hat{a}_{1var}^2}$.

2) The DTPS structure: Using the received signals in (15), one has

$$\hat{g_2} = \frac{\sqrt{\frac{P_{r2}}{{d_{rd}}^e}}}{\sqrt{\frac{\hat{P_{r2}}}{{d_{rd}}^e}}} g_2 + \varepsilon_{22} \tag{27}$$

where $\varepsilon_{22} = \frac{\Sigma_{i_{22}=1}^{m_{21}} n_{22}[i_{22}]}{m_{21}\hat{a}_{2var}\sqrt{\frac{\hat{P_{r2}}}{{d_{rd}}^e}}}$ and $\hat{P_{r2}} = \frac{\eta P_{s2} |\hat{h_2}|^2 (1-\rho_d)(D-m_{21})}{D {d_{sr}}^e}$ from (12). Substituting (27) and (13) in (16), the end-to-end SNR can be derived as

$$\gamma_{2end} = \frac{\rho_d \frac{P_{s2}}{{d_{sr}}^e} |\hat{g_2}|^2 |\hat{h_2}|^2}{v_2} \tag{28}$$

where $v_2 = \rho_d \frac{P_{s2}}{{d_{sr}}^e} |\hat{g_2}|^2 \varepsilon_{21var} + |\hat{g_2}|^2 N_{21} + \rho_d \frac{P_{s2}}{{d_{sr}}^e} \varepsilon_{22var} |\hat{h_2}|^2 + \rho_d \frac{P_{s2}}{{d_{sr}}^e} \varepsilon_{21var}\varepsilon_{22var} + N_{21}\varepsilon_{22var} + \frac{N_{22}}{\frac{\hat{P_{r2}}}{{d_{rd}}^e} \hat{a}_{2var}^2}$.

3) The CPS structure: Using the received signal in (22), the channel gain of the RD link can be estimated as

$$\hat{g_3} = \frac{\sqrt{\frac{P_{r3}}{{d_{rd}}^e}}}{\sqrt{\frac{\hat{P_{r2}}}{{d_{rd}}^e}}} g_3 + \varepsilon_{32} \tag{29}$$

where $\varepsilon_{32} = \frac{\Sigma_{i_{32}=1}^{m_{31}} n_{32}[i_{32}]}{m_{31}\hat{a}_{3var}}$ is the estimation error and $\hat{P_{r3}} = \frac{\eta P_{s3} |h_3|^2 (1-\rho_c)}{{d_{sr}}^e}$ from (19).

Substituting (29) and (20) in (23), the end-to-end SNR can be derived from (23) as

$$\gamma_{3end} = \frac{|\hat{h_3}|^2 |\hat{g_3}|^2 \frac{P_{s3}}{{d_{sr}}^e}}{v_3} \tag{30}$$

where $v_3 = \frac{P_{s3}}{{d_{sr}}^e} |\hat{g_3}|^2 \varepsilon_{31var} + \frac{P_{s3}}{{d_{sr}}^e} \varepsilon_{32var} |\hat{h_3}|^2 + |\hat{g_3}|^2 N_{31} + \frac{P_{s3}}{{d_{sr}}^e} \varepsilon_{31var}\varepsilon_{32var} + \varepsilon_{32var} N_{31} + \frac{N_{32}}{\frac{\hat{P_{r2}}}{{d_{rd}}^e} \hat{a}_{3var}^2}$,$\varepsilon_{31var} = E\{|\varepsilon_1|^2\}$ and $\varepsilon_{32var} = E\{|\varepsilon_2|^2\}$.

IV. Achievable Rate and BER Analysis

In this section, we will first derive the CDF of the end-to-end SNR for the three novel structures in (26), (28), (30). Then, we will calculate the rate and BER.

1) The CEPS Structure: To derive the CDF, we first calculate $Var(\varepsilon_{11})$ and $Var(\varepsilon_{12})$. From (5), ε_{11} has a mean of zero, and a variance of

$$Var(\varepsilon_{11}) = E\{|\varepsilon_{11}|^2\} = \frac{N_{11}}{m_{11}\rho_p \frac{P_{s1}}{{d_{sr}}^e}}. \tag{31}$$

Similarly, ε_{12} has a mean of zero and a variance of

$$Var(\varepsilon_{12}) = \frac{N_{12}D\left(\frac{P_{s1}}{{d_{sr}}^e}|\hat{h_1}|^2 + N_{11}\right)}{[\eta \frac{P_{s1}}{{d_{sr}}^e}|\hat{h_1}|^2 (1-\rho_p)\, m_{11}]m_{11}}. \tag{32}$$

Assume that h_{sd} is estimated in a similar way, and the estimation error is ε_{sd}. One has

$$Var(\varepsilon_{sd}) = \frac{N_{sd}}{D\frac{P_{s1}}{{d_{sd}}^e}}. \tag{33}$$

Using (31) and (32) in (26), the end-to-end SNR of the relaying link can be derived as

$$\gamma_{1end} = \frac{|\hat{g_1}|^2 |\hat{h_1}|^2 \frac{P_{s1}}{{d_{sr}}^e}}{w_1} \tag{34}$$

where $w_1 = \frac{N_{11}|\hat{g_1}|^2}{m_{11}\rho_p} + |\hat{g_1}|^2 N_{11} + \frac{N_{12}N_{11}D\left(\frac{P_{s1}}{{d_{sr}}^e}|\hat{h_1}|^2+N_{11}\right)}{[\eta \frac{P_{s1}}{{d_{sr}}^e}|\hat{h_1}|^2(1-\rho_p)]{m_{11}}^2 m_{11}\rho_p} + \frac{\frac{P_{s1}}{{d_{sr}}^e}|\hat{h_1}|^2 N_{12}D\left(\frac{P_{s1}}{{d_{sr}}^e}|\hat{h_1}|^2+N_{11}\right)}{[\eta \frac{P_{s1}}{{d_{sr}}^e}|\hat{h_1}|^2(1-\rho_p)m_{11}]m_{11}} + \frac{N_{12}D\left(\frac{P_{s1}}{{d_{sr}}^e}|\hat{h_1}|^2+N_{11}\right)[\frac{N_{11}}{m_{11}}+1]}{[\eta \frac{P_{s1}}{{d_{sr}}^e}|\hat{h_1}|^2(1-\rho_p)m_{11}]}$.

The SNR of the direct link is

$$\gamma_{sd} = \frac{\frac{P_{s1}}{{d_{sd}}^e}|\hat{h_{sd}}|^2}{\frac{P_{s1}}{{d_{sd}}^e}Var(\varepsilon_{sd}) + N_{sd}} = \frac{\frac{P_{s1}}{{d_{sd}}^e}|\hat{h_{sd}}|^2}{\frac{N_{sd}}{D} + N_{sd}}. \tag{35}$$

To move forward, we need the distributions of $|\hat{h_1}|^2$, $|\hat{h_{sd}}|^2$ and $|\hat{g_1}|^2$. By using the expression of $\hat{h_1}$ in (5), its second-order moment can be derived as

$$\begin{aligned}
&E(|\hat{h_1}|^2) = E|h_1 + \frac{\Sigma_{i_{11}=1}^{m_{11}} n_{11}[i_{11}]}{m_{11}\sqrt{\rho_p \frac{P_{s1}}{{d_{sd}}^e}}}|^2 = E(|h_1|^2 \\
&+ |\frac{\Sigma_{i_{11}=1}^{m_{11}} n_{11}[i_{11}]}{m_{11}\sqrt{\rho_p \frac{P_{s1}}{{d_{sd}}^e}}}|^2 + 2Re\{h_1 \times \frac{\Sigma_{i_{11}=1}^{m_{11}} n_{11}[i_{11}]^*}{m_{11}\sqrt{\rho_p \frac{P_{s1}}{{d_{sd}}^e}}}\}) \\
&= E(|h_1|^2) + E\left(|\frac{\Sigma_{i_{11}=1}^{m_{11}} n_{11}[i_{11}]}{m_{11}\sqrt{\rho_p \frac{P_{s1}}{{d_{sd}}^e}}}|^2\right) \\
&= E(|h_1|^2) + |\frac{N_{11}}{{m_{11}}^2 \rho_p \frac{P_{s1}}{{d_{sd}}^e}}| \times m_{11} = 2\theta^2 + \frac{N_{11}}{m_{11}\rho_p \frac{P_{s1}}{{d_{sr}}^e}}
\end{aligned} \tag{36}$$

Since h_1 and ε_{11} are complex Gaussian, $\hat{h_1}$ is also complex Gaussian. Thus, $|\hat{h_1}|^2$ is an exponential random variable with scale parameter

$$\lambda_{11} = \frac{1}{2\theta^2 + \frac{N_{11}}{m_{11}\rho_p \frac{P_{s1}}{{d_{sr}}^e}}}. \tag{37}$$

The probability density function (PDF) of $|\hat{h_1}|^2$ can be written as

$$f_{|\hat{h_1}|^2}(x) = \lambda_{11} e^{-\lambda_{11}x}. \tag{38}$$

Its CDF is

$$F_{|\hat{h_1}|^2}(x) = 1 - e^{-\lambda_{11}x}. \tag{39}$$

Similarly, assuming that $E\left\{\frac{|h_1|^2}{|\hat{h_1}|^2}\right\} \approx \frac{E\{|h_1|^2\}}{E\{|\hat{h_1}|^2\}}$, we can get

$$\begin{aligned}
E\left(|\hat{g_1}|^2\right) \approx &\frac{4\theta^4}{2\theta^2 + \frac{|N_{11}|}{m_{11}\rho_p \frac{P_{s1}}{{d_{sr}}^e}}} + \frac{N_{12}D}{(m_{11})\eta(1-\rho_p)m_{11}} \\
&- \frac{N_{12}D}{\frac{P_{s1}}{{d_{sr}}^e}m_{11}\eta(1-\rho_p)m_{11}} \frac{N_{11}Ei(0)}{2\theta^2 + \frac{N_{11}}{(m_{11}\rho_p \frac{P_{s1}}{{d_{sr}}^e})}}
\end{aligned} \tag{40}$$

where $E[\frac{N_{11}}{|\hat{h_1}|^2}] = N_{11} \times \int_0^\infty \frac{1}{x}\lambda_{11}e^{-\lambda_{11}x}dx = -\frac{N_{11}}{m_{11}\rho_p \frac{P_{s1}}{{d_{sr}}^e}}Ei(0)$ has been used. When ε_{11} is small, $|\hat{g_1}|^2$ can be approximated as an exponential random variable. Therefore, let $\lambda_{12} = \frac{1}{\frac{4\theta^4}{2\theta^2 + \frac{|N_{11}|}{m_{11}\rho_p \frac{P_{s1}}{{d_{sr}}^e}}} + \frac{|N_{12}||D|\rho_p}{|m_{11}|\eta|1-\rho_p|m_{11}}}$. Its PDF can be approximated as

$$f_{|\hat{g_1}|^2}(x) = \lambda_{12} e^{-\lambda_{12}x} \tag{41}$$

and its CDF can be approximated as

$$F_{|\hat{g_1}|^2}(x) = 1 - e^{-\lambda_{12}x}. \tag{42}$$

Similarly, let $\lambda_{sd} = \frac{1}{2\theta^2 + \frac{N_{sd}}{D\frac{P_{s1}}{{d_{sd}}^e}}}$. The PDF and CDF of $|\hat{h_{sd}}|^2$ are

$$f_{|\hat{h_{sd}}|^2}(x) = \lambda_{sd} e^{-\lambda_{sd}x} \tag{43}$$

and

$$F_{|\hat{h_{sd}}|^2}(x) = 1 - e^{-\lambda_{sd}x}. \tag{44}$$

The CDF of the relaying link can then be derived using these exprerssions in Appendix A as

$$\begin{aligned}
F_{\gamma_{1end}}(\gamma_{01}) = 1 - &\frac{1}{\frac{P_{s1}}{{d_{sr}}^e}\left(2\theta^2 + |\frac{N_1}{m_{11}\rho_p \frac{P_{s1}}{{d_{sr}}^e}}|\right)} \\
&e^{-\frac{\gamma_{01}N_1 + \gamma_{01}N_1 m_{11}\rho_p}{2\theta^2 m_{11}\rho_p \frac{P_{s1}}{{d_{sr}}^e} + |N_1|}} \frac{2\theta^2 m_{11}\rho_p \frac{P_{s1}}{{d_{sr}}^e} + |N_1|}{m_{11}\rho_p} - \\
&\frac{e^{-\frac{\lambda_{12}m_{11}\gamma_{01}N_{12}\rho_p D}{\eta\rho_p m_{11}(1-\rho_p){m_{11}}^2 \frac{P_{s1}}{{d_{sr}}^e}y} - \frac{\gamma_{01}N_1 + \gamma_{01}N_1 m_{11}}{2\theta^2 m_{11}\rho_p \frac{P_{s1}}{{d_{sr}}^e} + |N_1|}}}{\left(2\theta^2 + |\frac{N_1}{m_{11}\rho_p \frac{P_{s1}}{{d_{sr}}^e}}|\right)} \\
&\frac{2}{\frac{P_{s1}}{{d_{sr}}^e}}\left(\frac{z_1(\gamma_{01})}{(\eta m_{11}(1-\rho_p){m_{11}}^2)m_{11}\rho_p}\right)^{\frac{1}{2}} K_1\left(2\sqrt{\frac{z_2(\gamma_{01})}{w_4}}\right).
\end{aligned} \tag{45}$$

The CDF of the direct link can calculated as

$$F_{\gamma_{sd}}(\gamma_{01}) = 1 + (\lambda_{sd} - 1)e^{-\lambda_{sd}\left(\frac{N_{sd}\gamma_{th}{d_{sd}}^e}{DP_{s1}} + \frac{\gamma_{th}N_{sd}{d_{sd}}^e}{P_{s1}}\right)}. \tag{46}$$

Thus, the achievable rate without direct link can be derived as

$$AR_1 = [1 - F_{\gamma_{1end}}(\gamma_{01})] \times \frac{D - m_{11}}{D}. \tag{47}$$

and the achievable rate with a direct link can be derived as

$$AR_{1d} = [1 - F_{\gamma_{sd}}(\gamma_{01})F_{\gamma_{1end}}(\gamma_{01})] \times \frac{D - m_{11}}{D}. \tag{48}$$

Moreover, the bit-error-rate (BER) without direct link can be calculated as

$$\begin{aligned} BER_1 &= \int_0^\infty \frac{1}{2} erfc(\sqrt{x}) * dF_{\gamma_{1end}}(x) \\ &= \frac{1}{2}\int_0^\infty \frac{e^{-x}}{\sqrt{x*\pi}} F_{\gamma_{1end}}(x)dx. \end{aligned} \tag{49}$$

and the BER with direct link can be calculated as

$$\begin{aligned} BER_{1d} &= \int_0^\infty \frac{1}{2} erfc(\sqrt{x}) * d(F_{\gamma_{1end}}(x)F_{\gamma_{sd}}(x)) \\ &= \frac{1}{2}\int_0^\infty \frac{e^{-x}}{\sqrt{x*\pi}} F_{\gamma_{1end}}(x)F_{\gamma_{sd}}(x)dx. \end{aligned} \tag{50}$$

where $erfc(x)$ is the complementary error function.

2) The DTPS structure: Using similar methods, the CDF of γ_{2end} can be derived as

$$\begin{aligned} &F_{\gamma_{2end}}(\gamma_{02}) = 1 + (\rho_d - 1)e^{\frac{\gamma_{02}N_{21}\rho_d + \gamma_{02}N_{21}m_{21}}{2\theta^2\rho_d m_{21}P_{s2} + \rho_d N_{21}}} \\ &- e^{-\frac{\gamma_{02}N_{22}m_{21}D}{(\frac{4\theta^4}{2\theta^2 + \frac{|N_{21}|}{m_{21}\frac{P_{s2}}{d_{sr}{}^e}}} + \frac{N_{22}D}{[\eta(1-\rho_d)(D-m_{21})]m_{21}})\eta(1-\rho_d)(D-m_{21})m_{21}{}^2}} \\ &\frac{e^{-\frac{\gamma_{02}N_{21}\rho_d + \gamma_{02}N_{21}m_{21}}{2\theta^2\rho_d m_{21}\frac{P_{s2}}{d_{sr}{}^e} + |N_{21}\rho_d|}}}{\left(2\theta^2 + |\frac{N_{21}}{m_{21}\frac{P_{s2}}{d_{sr}{}^e}}|\right)} \frac{2}{\frac{P_{s2}}{d_{sr}{}^e}} (\frac{z_3(\gamma_{02})}{\eta(1-\rho_d)(D-m_{21})m_{21}^3})^{\frac{1}{2}} \\ &K_1(2\sqrt{\frac{z_4(\gamma_{02})}{w_5}}) \end{aligned} \tag{51}$$

where $w_5 = \eta(1-\rho_d)(D-m_{21})m_{21}^2$ $(2\theta^2 m_{21}\frac{P_{s2}}{d_{sr}{}^e}\rho_d + |N_{21}\rho_d|)$, $z_3(x) = \frac{1}{\frac{4\theta^4}{2\theta^2 + \frac{|N_{21}|}{m_{21}\frac{P_{s2}}{d_{sr}{}^e}}} + \frac{N_{22}D}{[\eta(1-\rho_d)(D-m_{21})]m_{21}}}$ $[xN_{21}N_{22}\rho_d D + xm_{21}N_{22}N_{21}D + xN_{22}m_{21}^2 D + xN_{22}m_{21}D * \frac{x\rho_d N_{21}}{m_{21}} + xN_{21}](2\theta^2 m_{21}\rho_d\frac{P_{s2}}{d_{sr}{}^e} + |N_{21}\rho_d|)$ and $z_4(x) = \frac{1}{\frac{4\theta^4}{2\theta^2 + \frac{|N_{21}|}{m_{21}\frac{P_{s2}}{d_{sr}{}^e}}} + \frac{N_{22}D}{[\eta(1-\rho_d)(D-m_{21})]m_{21}}}$ $(xN_{21}N_{22}\rho_d D + xm_{21}N_{22}N_{21}D + xN_{22}m_{21}^2 D + xN_{22}m_{21}D * \frac{x\rho_d N_{21}}{m_{21}} + xN_{21})m_{21}$.

Thus, the achievable rate without direct link can be derived as

$$AR_2 = [1 - F_{\gamma_{2end}}(\gamma_{02})] \times (\frac{D - m_{21}}{D}) \tag{52}$$

and the achievable rate with a direct link can be derived as

$$AR_{2d} = [1 - F_{\gamma_{2end}}(\gamma_{02})F_{\gamma_{sd}}(\gamma_{02})] \times (\frac{D - m_{21}}{D}). \tag{53}$$

The BER without direct link can be calculated as

$$BER_2 = \frac{1}{2}\int_0^\infty \frac{e^{-x}}{\sqrt{x*\pi}} F_{\gamma_{2end}}(x)dx. \tag{54}$$

and the BER with direct link can be calculated as

$$BER_2 = \frac{1}{2}\int_0^\infty \frac{e^{-x}}{\sqrt{x*\pi}} F_{\gamma_{2end}}(x)F_{\gamma_{sd}}(x)dx. \tag{55}$$

3) The CPS structure: Using similar methods, the CDF of γ_{3end} can be derived as

$$\begin{aligned} &F_{\gamma_{3end}}(\gamma_{03}) = 1 + (\rho_c - 1)e^{\frac{\frac{\gamma_{03}N_{31}}{\rho_c} + \gamma_{03}N_{31}m_{31}}{2\theta^2\rho_c m_{31}P_{s3} + N_{31}}} \\ &- \frac{1}{\left(2\theta^2 + |\frac{N_{31}}{m_{31}\rho_c\frac{P_{s3}}{d_{sr}{}^e}}|\right)} e^{-\frac{\lambda_{32}{}^b}{d} - \frac{\frac{\gamma_{03}N_{31}}{\rho_c} + \gamma_{03}N_{31}m}{2\theta^2\rho_c m_{31}\frac{P_{s3}}{d_{sr}{}^e} + |N_{31}|}} \\ &\frac{2}{\frac{P_{s3}}{d_{sr}{}^e}} (\frac{z_5(\gamma_{03})}{[\eta(1-\rho_c)(D-m_{31})]m_{31}^3})^{\frac{1}{2}} K_1(2\sqrt{\frac{z_6(\gamma_{03})}{w_6}}) \end{aligned} \tag{56}$$

where $w_6 = [\eta(1-\rho_c)(D-m_{31})m_{31}^2](2\theta^2\rho_c m_{31}\frac{P_{s3}}{d_{sr}{}^e} + |N_{31}|)$, $z_5(x) = \frac{1}{\frac{4\theta^4}{2\theta^2 + \frac{|N_{31}|}{m_{31}\rho_c\frac{P_{s3}}{d_{sr}{}^e}}} + \frac{\rho_c|N_{32}||D|}{|m_{31}|\eta|1-\rho_c|D}}$ $[xN_{31}N_{32}D + xm_{31}N_{32}N_{31}D + xN_{32}m_{31}^2 D + xN_{32}m_{31}D * \frac{xN_{31}}{\rho_c{}^2 m_{31}} + \frac{xN_{31}}{\rho_c}](2\theta^2 m_{31}\rho_c\frac{P_{s3}}{d_{sr}{}^e} + |N_{31}|)$ and $z_6(x) = \frac{1}{\frac{4\theta^4}{2\theta^2 + \frac{|N_{31}|}{m_{31}\rho_c\frac{P_{s3}}{d_{sr}{}^e}}} + \frac{\rho_c|N_{32}|}{|m_{31}|\eta|1-\rho_c|}}(xN_{31}N_{32}D + xmN_{32}N_{31}D + xN_{32}m_{31}^2 D + xN_{32}m_{31}D * \frac{xN_{31}}{\rho_c{}^2 m_{31}} + \frac{xN_{31}}{\rho_c})m_{31}$.

Thus, the achievable rate without direct link can be derived as

$$AR_3 = (1 - F_{\gamma_{3end}}(\gamma_{03})) \times (\frac{D - m_{31}}{D}) \tag{57}$$

and the achievable rate with a direct link can be derived as

$$AR_{3d} = (1 - F_{\gamma_{3end}}(\gamma_{03})F_{\gamma_{sd}}(\gamma_{03})) \times (\frac{D - m_{31}}{D}) \tag{58}$$

The BER without direct link can be calculated as

$$BER_3 = \frac{1}{2}\int_0^\infty \frac{e^{-x}}{\sqrt{x*\pi}} F_{\gamma_{3end}}(x)dx \tag{59}$$

and the BER with direct link can be calculated as

$$BER_{3d} = \frac{1}{2}\int_0^\infty \frac{e^{-x}}{\sqrt{x*\pi}} F_{\gamma_{3end}}(x)F_{\gamma_{sd}}(x)dx \tag{60}$$

The above derived expressions can be used to calculate the AR and BER for the three structures. All the BER results are one-dimensional integrals, which can be easily calculated using common mathematical software, ie., MATLAB. All the AR results are in closed-form. Next, we will provide some numerical examples.

V. NUMERICAL RESULTS AND DISCUSSION

In this section, we study the performances of the three novel structures in terms of achievable rate and bit-error-rate. In the study, we fix $\frac{P_{s1}}{d_{sr}{}^e} = \frac{P_{s2}}{d_{sr}{}^e} = \frac{P_{s2}}{d_{sr}{}^e} = 1$, $\eta = 0.5, D = 100, N_{11} = N_{12} = N_{21} = N_{22} = N_{31} = N_{32} = 1$. Define $\gamma_1 = \frac{|h|^2}{2\sigma^2}$ as the instantaneous SNR of the SR link, and $\gamma_2 = \frac{|g|^2}{2\sigma^2}$ as the instantaneous SNR of the RD link, where $g_1 = g_2 = g_3 = g$, $h_1 = h_2 = h_3 = h$. The values of g and h will change with γ_1 and γ_2, and their real and imaginary parts are the same.

Fig. 3 shows the outage probability of different structures by using simulation and analysis for comparison. One sees that there is an excellent match between simulation and analysis. This applies to all the following figures but to maintain the readability of the figures, simulation results are not shown, as they are not visible in 3D plots.

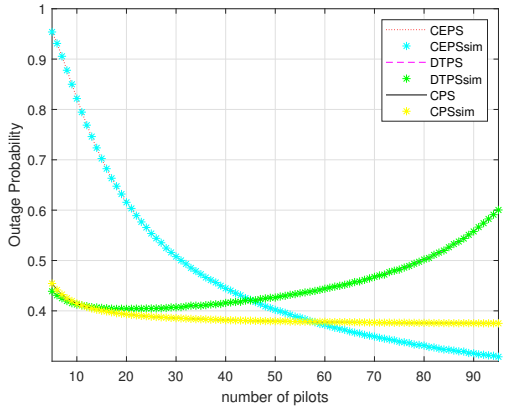

Fig. 3. Comparison of simulation and analysis, when γ_1 and γ_2 are fixed at 10 dB and 10 dB.

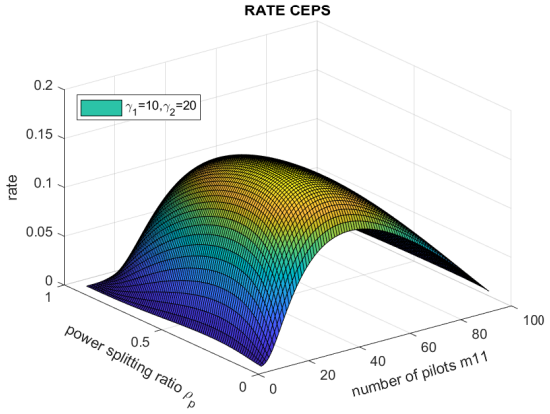

Fig. 5. Achievable rate of the CEPS structure versus the power splitting ratio ρ_p, when γ_1 and γ_2 are fixed at 10 dB and 20 dB.

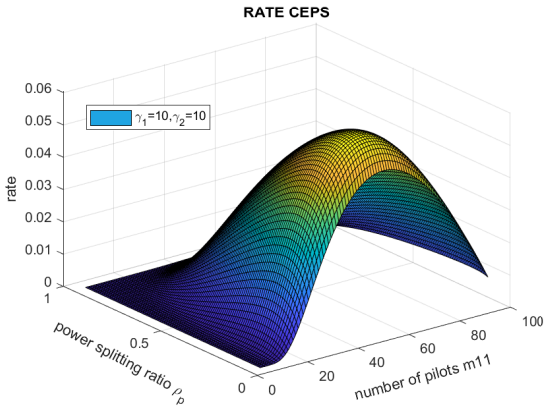

Fig. 4. Achievable rate of the CEPS structure versus the power splitting ratio ρ_p, when γ_1 and γ_2 are fixed at 10 dB and 10 dB.

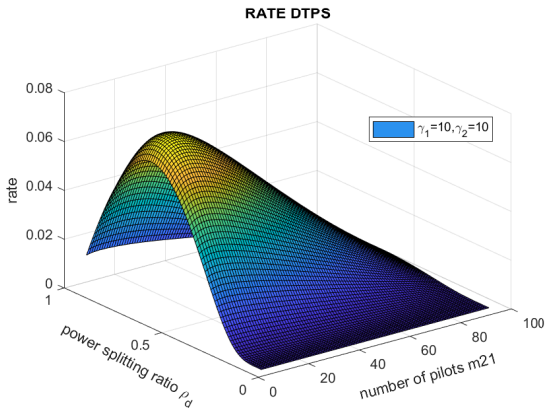

Fig. 6. Achievable rate of the DTPS structure versus the power splitting ratio ρ_d, when γ_1 and γ_2 are fixed at 10 dB and 10 dB.

A. Achievable Rate Analysis

Fig. 4 illustrates the achievable rate of the CEPS structure versus the power splitting ratio ρ_p, when γ_1 and γ_2 are fixed at 10 dB and 10 dB, respectively. The value of ρ_p is changing between 0 to 1 with an interval 0.05. The value of m_{11} is changing between 0 to 100 with an interval 1. First of all, we can see that the achievable rate increases first and then decreases when m_{11} or ρ_p increase. The peak point represents the optimal value. In this case, it can be observed that the optimal value is achieved at $m_{11} = 50$ and $\rho_p = 0.13$, and the maximum achievable rate is around 0.058. A larger m_{11} means more accurate estimate of $\hat{h}_1$, and more energy for harvesting but less time for data transmission. A larger ρ_p means more accurate estimate of $\hat{h}_1$, but less energy for harvesting. Thus, one must choose ρ_p carefully using our results to achieve the best performance.

Fig. 5 is similar to Fig. 4, expect that γ_1 , γ_2 are fixed at 10 dB and 20 dB, respectively. In this case, the rate increases in most cases. The optimal values are $m_{11} = 50$ and $\rho_p = 0.3$, and the maximum rate is around 0.116. Thus, the performance of the CEPS structure can be improved by increasing γ_2, but the optimal values change too.

Fig. 6 illustrates the achievable rate of the DTPS structure versus the number of pilots for m_{11} and ρ_d, when γ_1 , γ_2 are fixed at 10 dB and 10 dB. Again, we can see that the achievable rate increases first and then decreases when m_{21} or ρ_d increase, implying that the optimal value exists. For this structure, the optimal values are $m_{21} = 15$ and $\rho_d = 0.65$, and the maximum achievable rate is around 0.07.

Fig. 7 shows the rate of the CPS structure versus the number of pilots for m_{31} and ρ_c, when γ_1 , γ_2 are fixed at 10 dB and 10 dB. Similar observations can be made. The optimal values in Fig. 7 are $m_{31} = 20$ and $\rho_c = 0.65$ with a maximum rate of around 0.074.

By comparing the achievable rates of the three different structures, one can see that CEPS has a smaller maximum achievable rate than DTPS and CPS. Also, DTPS and CPS have similar optimal achievable rates from our calculations, and CPS has a slightly bigger maximum achievable rate than DTPS. Therefore, CPS has the best performance among these three structures, and CEPS has the worst.

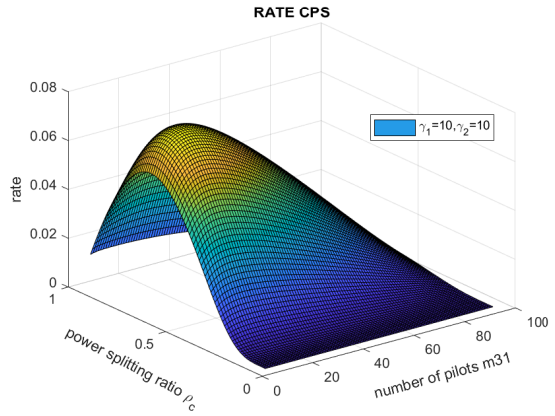

Fig. 7. Achievable rate of the CPS structure versus the power splitting ratio ρ_c, when γ_1 and γ_2 are fixed at 10 dB and 10 dB.

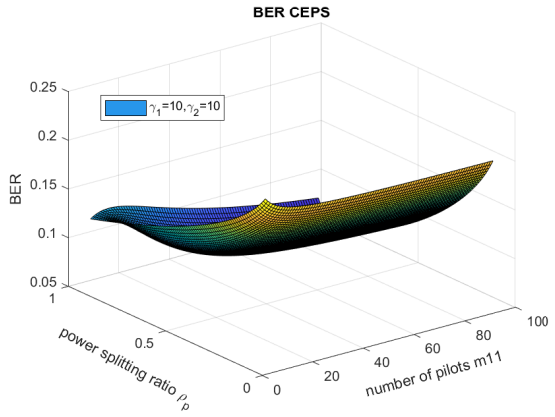

Fig. 8. BER of the CEPS structure versus the power splitting ratio ρ_p, when γ_1 and γ_2 are fixed at 10 dB and 20 dB.

B. Bit Error Rate Analysis

Fig. 8 illustrates the BER of the CEPS structure, when γ_1 and γ_2 are fixed at 10 dB and 10 dB, respectively. In this case, we can see that the BER decreases first and then rises up when m_{11} or ρ_p increase. In this case, it can be observed that the optimal values are $m_{11} = 12$ and $\rho_p = 0.95$, and the minimum BER is around 0.07. Fig. 9 shows the BER of the DTPS structure, when γ_1 and γ_2 are fixed at 10 dB and 10 dB, respectively. In this case, it can observed that the optimal values are $m_{21} = 15$ and $\rho_d = 0.51$, and the minimum BER is around 0.0353. Fig. 10 illustrates the BER of the CPS structure, when γ_1 and γ_2 were fixed at 10 dB and 10 dB, respectively. In this case, it can be observed that the optimal value of ρ_c is 0.56 and m_{31} does not have optimal value, the minimize BER is around 0.03243.

Comparing the BERs of the three different structures, DTPS and CPS have similar optimal BER from our calculations, while CPS has minor improvement compared with DTPS. Therefore, CPS has the best performance among these three structures.

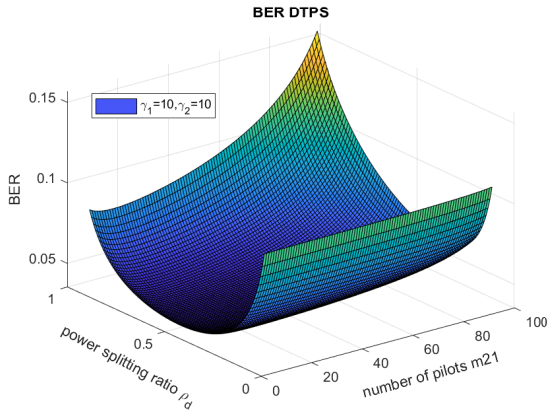

Fig. 9. BER of the DTPS structure versus the power splitting ratio ρ_d, when γ_1 and γ_2 are fixed at 10 dB and 20 dB.

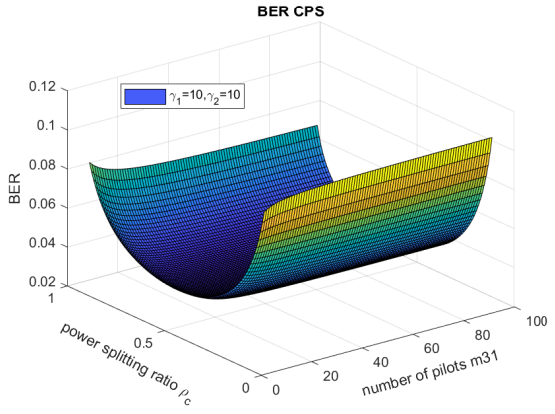

Fig. 10. BER of the CPS structure versus the power splitting ratio ρ_c, when γ_1 and γ_2 are fixed at 10 dB and 20 dB.

C. Effect of Direct link

In this part, we compare the performance of CEPS with and without a direct link. The DTPS and CPS has same observation and are not shown here. Fig. 11 compares the performances with and without direct link for different power splitting ratios of 0.4 and 0.8. The achievable rate is higher with direct link, as expected.

D. Comparison with Previous works

Fig. 12 compares the BERs of our combination structures with the basic time-switching AF relaying (TSAF) structure in the literature. The BER values of all three new structures are smaller than that of TS. Therefore, our novel structures have better performance than the conventional TS structures in previous works.

VI. Conclusion

Three novel combination structures for energy harvesting AF relaying have been investigated in this paper. Both distance and direct link have been considered, and the improvement of TS and PS energy harvesting protocols with different combinations has been discussed. Numerical results have verified

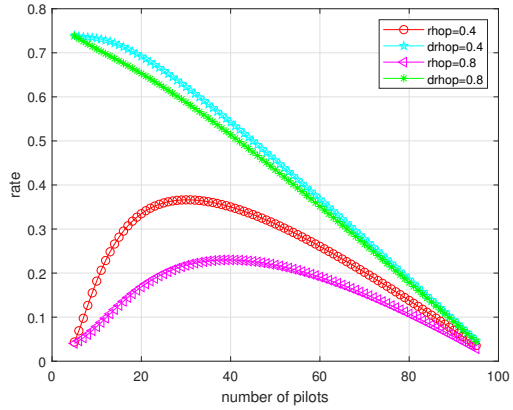

Fig. 11. Achievable rate of CEPS with and without direct link, when γ_1 and γ_2 are fixed at 10dB and 10dB.

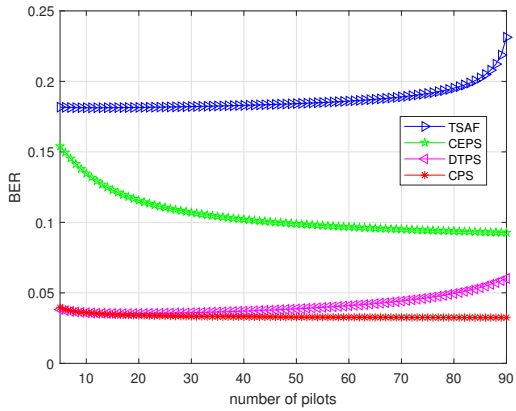

Fig. 12. Performance comparison between Novel structures and basic TS structure

the existence of optimal number of pilots and optimal value of power splitting ratio for channel estimation, data transmission and energy harvesting, when the packet size is fixed.

REFERENCES

[1] X. Lu, P. Wang, D. Niyato, D. I. Kim, and Z. Han, "Wireless networks with rf energy harvesting: A contemporary survey," *IEEE Communications Surveys and Tutorials*, vol. 17, no. 2, pp. 757–789, 2015.

[2] A. A. Nasir, X. Zhou, S. Durrani, and R. A. Kennedy, "Relaying protocols for wireless energy harvesting and information processing," *IEEE Transactions on Wireless Communications*, vol. 12, no. 7, pp. 3622–3636, 2013.

[3] Y. Chen, "Energy-harvesting af relaying in the presence of interference and nakagami-m fading," *IEEE Transactions on Wireless Communications*, vol. 15, no. 2, pp. 1008–1017, 2016.

[4] Q. Wu, M. Tao, D. W. K. Ng, W. Chen, and R. Schober, "Energy-efficient resource allocation for wireless powered communication networks," *IEEE Transactions on Wireless Communications*, vol. 15, no. 3, pp. 2312–2327, 2016.

[5] K. Xiong, P. Fan, C. Zhang, and K. B. Letaief, "Wireless information and energy transfer for two-hop non-regenerative mimo-ofdm relay networks," *IEEE Journal on Selected Areas in Communications*, vol. 33, no. 8, pp. 1595–1611, 2015.

[6] Y. Chen, "Energy-harvesting af relaying in the presence of interference and nakagami-m fading," *IEEE Transactions on Wireless Communications*, vol. 15, no. 2, pp. 1008–1017, 2016.

[7] B. Li, Z. Fei, and H. Chen, "Robust artificial noise-aided secure beamforming in wireless-powered non-regenerative relay networks," *IEEE Access*, vol. 4, pp. 7921–7929, 2016.

[8] B. Li, Z. Fei, Z. Chu, and Y. Zhang, "Secure transmission for heterogeneous cellular networks with wireless information and power transfer," *IEEE Systems Journal*, 2017.

[9] Y. Chen, K. T. Sabnis, and R. A. Abd-Alhameed, "New formula for conversion efficiency of rf eh and its wireless applications," *IEEE Transactions on Vehicular Technology*, vol. 65, no. 11, pp. 9410–9414, 2016.

[10] P.-V. Mekikis, A. Antonopoulos, E. Kartsakli, A. S. Lalos, L. Alonso, and C. Verikoukis, "Information exchange in randomly deployed dense wsns with wireless energy harvesting capabilities," *IEEE Transactions on Wireless Communications*, vol. 15, no. 4, pp. 3008–3018, 2016.

[11] S. Bi, Y. Zeng, and R. Zhang, "Wireless powered communication networks: An overview," *IEEE Wireless Communications*, vol. 23, no. 2, pp. 10–18, 2016.

[12] Y. Chen, W. Feng, R. Shi, and N. Ge, "Pilot-based channel estimation for af relaying using energy harvesting," *IEEE Transactions on Vehicular Technology*, vol. 66, no. 8, pp. 6877–6886, 2017.

[13] J.-M. Kang, I.-M. Kim, and D. I. Kim, "Wireless information and power transfer: Rate-energy tradeoff for nonlinear energy harvesting," *IEEE Transactions on Wireless Communications*, vol. 17, no. 3, pp. 1966–1981, 2018.

[14] X. Zhou, R. Zhang, and C. K. Ho, "Wireless information and power transfer: Architecture design and rate-energy tradeoff," *IEEE Transactions on communications*, vol. 61, no. 11, pp. 4754–4767, 2013.

[15] J. Ma, S. Zhang, H. Li, N. Zhao, and A. Nallanathan, "Iterative lmmse individual channel estimation over relay networks with multiple antennas," *IEEE Transactions on Vehicular Technology*, vol. 67, no. 1, pp. 423–435, 2018.

[16] D. Han, Y. Mo, J. Wu, S. Weerakkody, B. Sinopoli, and L. Shi, "Stochastic event-triggered sensor schedule for remote state estimation," *IEEE Transactions on Automatic Control*, vol. 60, no. 10, pp. 2661–2675, 2015.

[17] F. A. Khan, Y. Chen, and M.-S. Alouini, "Novel receivers for af relaying with distributed stbc using cascaded and disintegrated channel estimation," *IEEE Transactions on Wireless Communications*, vol. 11, no. 4, pp. 1370–1379, 2012.

[18] H. Yomo and E. D. Carvalho, "A csi estimation method for wireless relay network," *IEEE Communications letters*, vol. 11, no. 6, pp. 480–482, 2007.

[19] Y. Zhou and Y. Chen, "Performance analysis of end-to-end snr estimators for af relaying," *Telecommunication Systems*, pp. 1–12, 2017.

[20] A. Zafar, R. M. Radaydeh, Y. Chen, and M.-S. Alouini, "Enhancing the efficiency of constrained dual-hop variable-gain af relaying under nakagami-m fading," *IEEE Transactions on Signal Processing*, vol. 62, no. 14, pp. 3616–3630, 2014.

[21] A. Hussain, K. Lee, S.-H. Kim, S.-H. Chang, and D. I. Kim, "Performance analysis of dual-hop variable-gain relaying with beamforming over κ–μ fading channels," *IET Communications*, vol. 11, no. 10, pp. 1587–1593, 2017.

APPENDIX A
PROOF OF CEPS

One has

$$I_{11} = P_{r1}\{\frac{P_{s1}}{d_{sr}{}^{e}}|\hat{h_1}|^2 - \frac{xN_{11}}{m_{11}\rho_p} - xN_{11} < 0\} \tag{61}$$

$$I_{12} = P_{r1}\{|\hat{g_1}|^2 < \frac{z}{w_2}|\left(\frac{P_{s1}}{d_{sr}{}^{e}}|\hat{h_1}|^2 - \frac{xN_{11}}{m_{11}\rho_p} - xN_{11}\right) > 0\} \tag{62}$$

where $w_2 = [\eta\rho_p m_{11}(1-\rho_p)m_{11}{}^2\frac{P_{s1}}{d_{sr}{}^{e}}|\hat{h_1}|^2](\frac{P_{s1}}{d_{sr}{}^{e}}|\hat{h_1}|^2 - \frac{xN_{11}}{m_{11}\rho_p} - xN_{11})$ and $z = xN_{12}N_{11}D\left(\frac{P_{s1}}{d_{sr}{}^{e}}|\hat{h_1}|^2 + N_{11}\right)$
$+ m_{11}x\rho_p N_{12}N_{11}D\left(\frac{P_{s1}}{d_{sr}{}^{e}}|\hat{h_1}|^2 + N_{11}\right)$
$+ xm_{11}m_{11}\rho_p N_{12}D\left(\frac{P_{s1}}{d_{sr}{}^{e}}|\hat{h_1}|^2 + N_{11}\right)$
$+ m_{11}\rho_p x\frac{P_{s1}}{d_{sr}{}^{e}}|\hat{h_1}|^2 N_{12}D\left(\frac{P_{s1}}{d_{sr}{}^{e}}|\hat{h_1}|^2 + N_{11}\right)$. Using the CDF of $|\hat{h_1}|^2$ in (36), one has

$$I_{11} = 1 - e^{-\frac{\frac{xN_{11}}{m_{11}\rho_p\frac{P_{s1}}{d_{sr}{}^{e}}} + \frac{xN_{11}}{\frac{P_{s1}}{d_{sr}{}^{e}}}}{2\theta^2 + |\frac{N_{11}}{m_{11}\rho_p\frac{P_{s1}}{d_{sr}{}^{e}}}|}}. \tag{63}$$

Also, (42) can be solved by using the CDF of $|\hat{g_1}|^2$ as

$$I_{12}=\int_{\frac{xN_{11}}{m_{11}\rho_p\frac{P_{s1}}{{d_{sr}}^e}}+\frac{xN_{11}}{\frac{P_{s1}}{{d_{sr}}^e}}}^{\infty}F_{|\hat{g_1}|^2}(\frac{z}{w_3})f_{|\hat{h_1}|^2}(y)dy \tag{64}$$

where $w_3=[\eta\rho_p m_{11}(1-\rho_p){m_{11}}^2\frac{P_{s1}}{{d_{sr}}^e}y]$ $(\frac{P_{s1}}{{d_{sr}}^e}y-\frac{xN_{11}}{m_{11}\rho_p}-xN_{11})$. Let $\frac{P_{s1}}{{d_{sr}}^e}y-\frac{xN_{11}}{m_{11}\rho_p}-xN_{11}=t$. By using this variable transformation, one has

$$I_{12}=\frac{1}{\frac{P_{s1}}{{d_{sr}}^e}\left(2\theta^2+|\frac{N_{11}}{m_{11}\rho_p\frac{P_{s1}}{{d_{sr}}^e}}|\right)}e^{-\frac{xN_{11}+xN_{11}m_{11}\rho_p}{2\theta^2 m_{11}\rho_p\frac{P_{s1}}{{d_{sr}}^e}+|N_{11}|}}$$
$$\frac{2\theta^2 m_{11}\rho_p\frac{P_{s1}}{{d_{sr}}^e}+|N_{11}|}{m_{11}\rho_p}-\frac{1}{\left(2\theta^2+|\frac{N_{11}}{m_{11}\rho_p\frac{P_{s1}}{{d_{sr}}^e}}|\right)} \tag{65}$$
$$e^{-\frac{\lambda_{12}m_{11}xN_{12}\rho_p D}{\eta\rho_p m_{11}(1-\rho_p){m_{11}}^2\frac{P_{s1}}{{d_{sr}}^e}y}-\frac{xN_{11}+xN_{11}m_{21}}{2\theta^2 m_{11}\rho_p\frac{P_{s1}}{{d_{sr}}^e}+|N_{11}|}}$$
$$\frac{2}{\frac{P_{s1}}{{d_{sr}}^e}}(\frac{z_1(x)}{(\eta m_{11}\,(1-\rho_p)\,{m_{11}}^2)m_{11}\rho_p})^{\frac{1}{2}}K_1(2\sqrt{\frac{z_2(x)}{w_4}})$$

where $w_4=(\eta m_{11}\,(1-\rho_p)\,{m_{11}}^2)(2\theta^2 m_{11}\rho_p\frac{P_{s1}}{{d_{sr}}^e}+|N_1|)$, $z_1(x)=(\frac{1}{\frac{4\theta^4}{2\theta^2+\frac{|N_1|}{m_{11}\rho_p\frac{P_{s1}}{{d_{sr}}^e}}}+\frac{|N_{12}||D|\rho_p}{|m_{11}|\eta|1-\rho_p|m_{11}}})$ $(xN_{12}N_1D+m_{11}\rho_p xN_{12}N_1D+xm_{11}m_{11}\rho_p N_{12}D+m_{11}xN_{12}D*\frac{xN_1\rho_p}{m_{11}\rho_p}+xN_1\rho_p)$ $(2\theta^2 m_{11}\rho_p\frac{P_{s1}}{{d_{sr}}^e}+|N_1|)$ and $z_2(x)=(\frac{1}{\frac{4\theta^4}{2\theta^2+\frac{|N_1|}{m_{11}\rho_p\frac{P_{s1}}{{d_{sr}}^e}}}+\frac{|N_{12}||D|\rho_p}{|m_{11}|\eta|1-\rho_p|m_{11}}})$ $(xN_{12}N_1D+m_{11}\rho_p xN_{12}N_1D+xm_{11}m_{11}\rho_p N_{12}D+m_{11}xN_{12}D*\frac{xN_1\rho_p}{m_{11}\rho_p}+xN_1\rho_p)m_{11}\rho_p$.

Ynlin Zhou received the M.S. degree from the School of Engineering, University of Warwick, U.K., in 2016. He is currently pursuing the Ph.D. degree at School Engineering in University of Warwick, U.K, from Feb. 2016. His research interest include energy harvesting, channel estimation and wireless relaying.

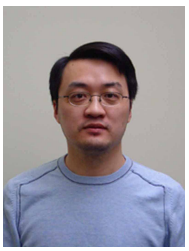

Yunfei Chen (S'02-M'06-SM'10) received his B.E. and M.E. degrees in electronics engineering from Shanghai Jiaotong University, Shanghai, P.R.China, in 1998 and 2001, respectively. He received his Ph.D. degree from the University of Alberta in 2006. He is currently working as an Associate Professor at the University of Warwick, U.K. His research interests include wireless communications, cognitive radios, wireless relaying and energy harvesting.